Bioorganic & Medicinal Chemistry 28 (2020) 115461

Contents lists available at ScienceDirect

Bioorganic & Medicinal Chemistry

journal homepage: www.elsevier.com/locate/bmc

New CDK8 inhibitors as potential anti-leukemic agents – Design, synthesis and biological evaluation

Eirik Solum[a,b,*], Trond Vidar Hansen[b], Reidun Aesoy[c], Lars Herfindal[c]

[a] Faculty of Health Sciences, Nord University, 7801 Namsos, Norway
[b] University of Oslo, PO Box 1068 Blindern, N-0316 Oslo, Norway
[c] Centre for Pharmacy, Department of Clinical Science, University of Bergen, PO Box 7800, N-5007 Bergen, Norway

ARTICLE INFO

Keywords:
CDK8 inhibition
Anti-leukemia
Steroids

ABSTRACT

Cyclin-dependent kinase 8 (CDK8) plays a vital role in regulating cell transcription either through its association with the mediator complex or by the phosphorylation of transcription factors. CDK8-mediated activation of oncogenes has proved to be important in a variety of cancer types including hematological malignancies. We have designed and synthesized a series of new synthetic steroids. The compounds were evaluated as CDK8 inhibitors *in vitro*. The three most potent compounds exhibit K_d-values towards CDK8 in the low nanomolar range (3.5–18 nM). Furthermore, the compounds displayed selectivity for CDK8 in a panel of 465 different kinases. The cell studies indicated a selectivity to kill AML-cancer cell lines compared to normal cell lines.

1. Introduction

Cyclin-dependent kinases (CDKs) are a family of serine/threonine protein kinases that control critical regulatory events during cell cycle and transcription.[1] Given these fundamental roles, it is unsurprising that deregulation of CDKs is a common feature of many cancers. In particular, Cyclin-dependent kinase 8 (CDK8), a ubiquitously expressed, primarily transcriptional member of the CDK family, has come under focus owing to investigations of its central roles in transcription and oncogenesis.[2–4] Several genetic and biochemical studies have established CDK8 as a key oncogenic driver in a variety of different cancer forms like colon cancer[5], prostate cancer[6] and melanoma[7]. It is also reported that a striking correlation exists between the expression of CDK8 and the duration of relapse-free survival in patients with breast- and ovarian cancer[8]. For example, breast cancer patients with below-median expression of CDK8 survive without the disease approximately seven years longer than patients with an above-median expression of CDK8.[9] From a biochemical perspective, CDK8 plays an important role in regulating transcription either through its association with the mediator complex or by phosphorylating transcription factors. Specifically, CDK8-mediated activation of oncogenic Wnt-β-catenin signaling, transcription of estrogen-inducible genes and suppression of super enhancer-associated genes contribute to oncogenesis in colorectal-, mammary- and hematological malignancies, respectively. Inhibitors of CDK8 have also been shown to be active in AML cells that have high activation of the signal transducer and activator of transcription 5 (STAT5).[10] STAT5 mediates several malignant properties in AML cells. Inhibition of STAT5 phosphorylation, through inhibition of for instance Flt3 or PIM-kinases, has shown therapeutic value.[11,12] Another aspect with CDK8 in cancer is that it is involved in tumor surveillance of NK-cells. Inhibition of CDK8 is known to increase NK cell cytotoxicity towards cancer cells.[13,14] The use of CDK8 inhibitors can therefore have a double action: First, by acting directly on the cancer cells, and secondly indirectly by activation the NK cells to more efficiently lyse the cancer cells. Hence, an interest to develop compounds inhibiting CDK8 has increased. As of today, based on high throughput screening (HTS) and computational methods towards different kinase panels, a few compounds have appeared as either CDK8 ligands or inhibitors.[15–18] (Fig. 1).

In 2012, the senexin compounds, exemplified by Senexin A (1) Fig. 1, were revealed as a class of selective CDK8 inhibitors. This group of compounds was discovered using HTS with more than 100,000 compounds for the downstream inhibition of p21-activation transcription. An optimization of the compounds led to Senexin A that was characterized as a kinase inhibitor with K_d = 0.83 μM and K_d = 0.31 μM for CDK8 and its structural homolog CDK19, respectively. The kinase activity of CDK8 was inhibited with an IC_{50} = 0.28 μM. Cortistatin A (**2**) is a naturally occurring steroidal alkaloid isolated from the marine sponge *Corticum simplex*.[19] It was reported in 2009 that **2** is a high-affinity binder, with K_d = 17 nM,

* Corresponding author.
E-mail address: eirik.j.solum@nord.no (E. Solum).

https://doi.org/10.1016/j.bmc.2020.115461
Received 19 February 2020; Received in revised form 17 March 2020; Accepted 22 March 2020
Available online 27 March 2020

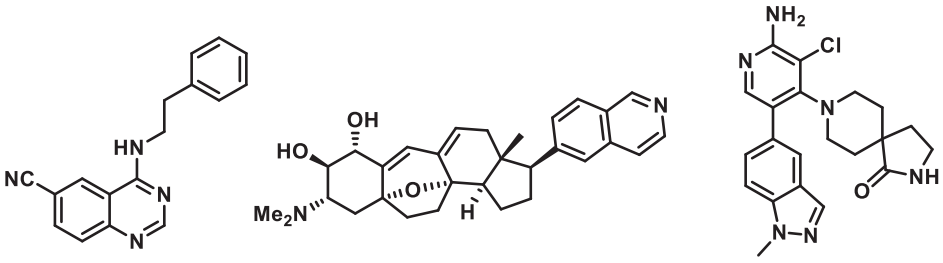

Senexin A (**1**) Cortistatin A (**2**) CCT251921 (**3**)

Fig. 1. Example of reported CDK8 inhibitors.

towards CDK8.[20] In addition to its strong binding affinity, the compound showed a high level of selectivity for CDK8. Cortistatin A was tested at 10 μM in a high-throughput binding assay against a panel 359 non-mutant kinases, and the calculated selectivity score at 35% control activity S(35)[21], proved to be 0,045. The authors suggested in a binding model that hydrogen bonding between the nitrogen on the isoquinoline side chain to Ala100 in CDK8 was important.[20] More recently, structural and mechanistic studies have revealed that compound **2** is a highly potent, ATP-competitive, CDK8 inhibitor, and utilizes its isoquinoline moiety to bind to the kinase hinge segment through the nitrogen of the isoquinoline and the N—H of Ala100. The steroidal-like core makes extensive contacts with the ATP-binding cavity.[22] Furthermore, the study investigated the potential of cortistatin A (**2**) as a treatment for acute myeloid leukemia (AML) and a 71% tumor growth inhibition on day 33, in mice containing SET-2 AML xenograft tumors, was reported. Importantly, cortistatin A had an acceptable pharmacokinetic profile in mice for once-daily *intraperitoneal* dosing and the reduction in the progression of the disease was reported to be dose-dependent.

The heterocyclic compound CCT251921 (**3**) was originally identified as a potent inhibitor of the Wnt signaling pathway.[23] A follow-up study using a chemical proteomics-based approach identified CDK8/CDK19 as its primary targets.[24] The compound was claimed to be selective for CDK8/CDK19 in a panel of 279 kinases at 1.0 μM; however CDK8 itself was not included in the panel as a positive control. Preclinical testing of these compounds showed that the compound inhibited Wnt-dependent activity in a number of colorectal cell lines, as well as the phosphorylation of the transcription factor Signal transducer and activator of transcription 1 (STAT1) at Ser727. The binding mode of CCT251921 (**3**) to CDK8 revealed that its pyridine nitrogen interacted with the kinase hinge segment by a similar interaction to the N—H of Ala100 as that of the isoquinoline nitrogen of cortistatin A (**2**). From this interaction, the indazole substituent of **3** is orientated towards the ATP-binding cavity in similarity to the steroidal core of cortistatin A. Additionally, the chlorine-atom, attached to the pyridine ring, in a *meta*-relationship to both the nitrogen atom and the indazole, further increased the affinity of compound **3** by an interaction with Phe97. In connection with our interest and earlier efforts in using steroids as lead compounds for the development of new anti-cancer agents,[25–30] we present our experimental approach by taking advantage of this information in the design of easily accessible steroid-based inhibitors of CDK8.

2. Results and discussion

2.1. Chemistry – Design and synthesis

In March 2018, Hatcher and coworkers demonstrated that several steroidal cortistatin A (**2**) analogs were effective inhibitors of CDK8.[31] In this work, we aim to advance their approach further by combining information of the binding modes of the pyridine core of CCT251921 (**3**) and the isoquinoline of cortistatin A (**2**). Compared to the work published by Hatcher and coworkers, we have included several more isoquinolinyl-, as well as pyridinyl and indolyl substituents attached to the unsaturated carbon 17 at the steroidal core. Encouraged by the work of Baran and coworkers and to simplify the SAR-studies,[32] we choose not to reduce the double bond on the D-ring of the analogs. Furthermore, the orientation of dimethylamino group of Cortistatin A is maintained in our analogs at the carbon number of the steroid nucleus. By this approach, several analogs have been made (see Scheme 1).

The synthesis of compounds **8–17** commenced with a Mitsunobu-type inversion of the chiral center at C-3 of epiandrosterone (**4**) to the corresponding androsterone-3-azide **5** using triphenylphosphine, diisopropyl azodicarboxylate (DIAD) and diphenylphosphorylazide (DPPA) in THF, from which androsterone-3-azide **5** was isolated in 73% yield. Then, in a one-pot sequence, a modified Staudinger reaction using trimethylphosphine in THF was employed to afford the intermediate steroidal amine, which was further converted to the dimethyl amine **6**, by an Eschweiler-Clarke type reaction[33–35] The enol-triflate **7** was made from the ketone **6** in a reaction using *N*-phenyl-bis(trifluoromethanesulfonimide) in the presence of NaHMDS at −78 °C. The key intermediate **7** was further converted to the desired compounds **8–17** using the Suzuki-Miyaura cross-coupling reaction with different boronic acids as coupling partners. Tetrakis(triphenylphosphine)palladium and caesium carbonate in THF/H_2O (1:1) enabled the preparation of compounds **8–17** in 31–42% overall yield (see Fig 2).

2.2. CDK8 profiling

Compounds **8–17** were tested for their ability to inhibit probe binding to protein kinase CDK8 *in vitro* at 50 nM concentration. In this assay, the ability of a test compound to compete with an immobilized, active site directed ligand is quantitatively measured and reported as percent of DMSO control (POC), with lower numbers indicating higher binding affinity. The results are displayed in Table 1. Except for **16**, all compounds displayed inhibitory activity towards CDK8 at 50 nM concentration. For the five most promising compounds, their K_d-values were determined. The most potent compound, the 5-isoquinoline analog **12**, inhibited CDK8 with a K_d = 3.5 nM, which is 3–4 times lower than the reported K_d-value of our lead compound cortistatin A (**2**) (17 nM) in a similar assay.[20] Compound **12** has a 5-isoquinoline substituent in the 17-position of the steroid core skeleton. For compound **9**, with a 5-chloropyridin-3-yl substituent as in CCT251921 (**3**), the K_d-value was determined to 13 nM in the same range as for cortistatin A (**2**).

To evaluate the kinase selectivity, we performed a KinomeScan™ binding analysis against a near comprehensive panel of 468 kinases at a concentration of 50 nM (Fig. 3). This profiling revealed selectivity of compounds **12** and **9** for CDK8, both with selectivity scores, S(10) at 0.01.[21] Furthermore, compound **14** displayed a K_d = 18 nM and a S(10)

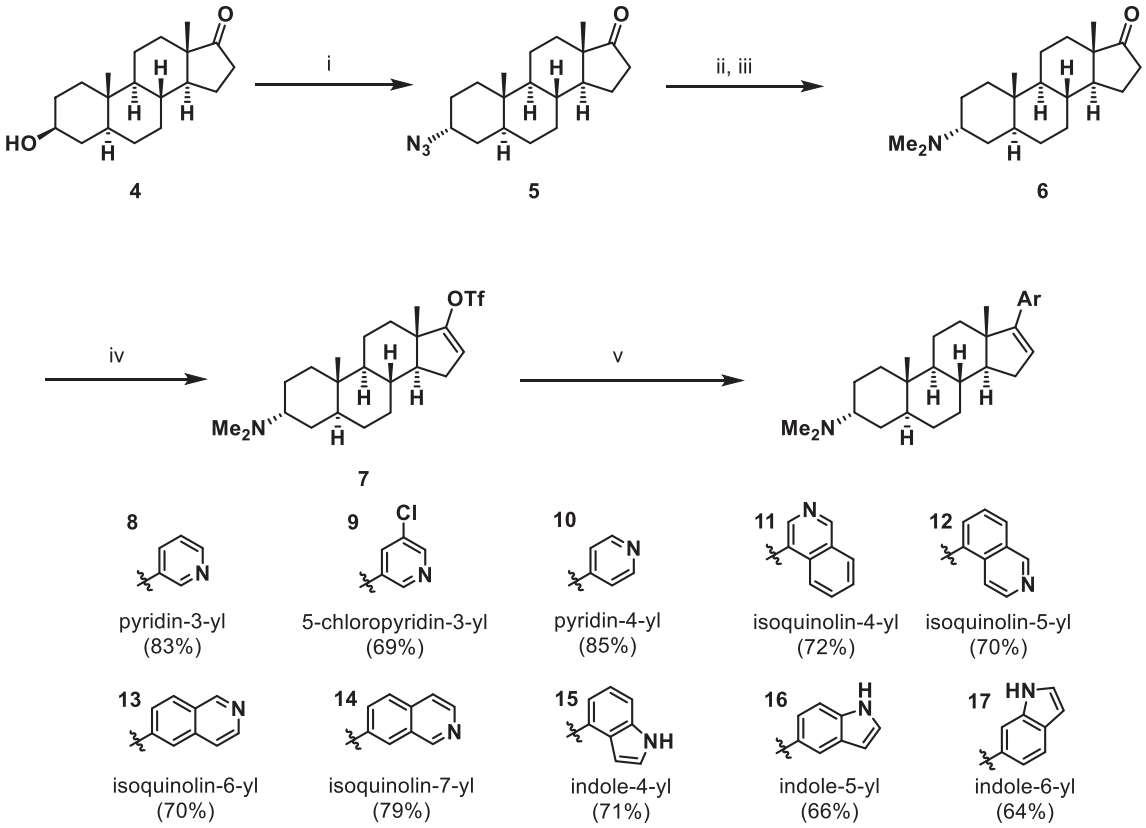

Scheme 1. Synthesis of compounds **8–17**. Reagents and conditions: i) PPh_3, DIAD, diphenyl phosphoryl azide, THF, rt, 10 h, 73%; ii) $P(CH_3)_3$, 1 M NaOH, THF, rt., 2 h; iii) AcOH, CH_2O, $NaCNBH_3$, MeOH, rt. 1 h, 73%; iv) NaHMDS, $PhN(SO_2CF_3)_2$, THF, −78 °C, 4 h, 85%; v) $ArB(OH)_2$, Cs_2CO_3, $Pd(Ph_3P)_4$, THF:H_2O (1:1) 60 °C, 5 h, 64–85%.

score of 0.01. These results are in line with the data presented by Hatcher and coworkers in their report from 2018, in which they measured the IC_{50} values of 18–24 nM and S(10) score of around 0.01 for a related compounds carrying isoquinolin-7-yl substituents on the steroid skeleton.[31]

2.3. In vitro studies

In order to assess whether the analogs could be lead compounds in acute myeloid leukemia (AML) therapy, we tested them against three cell lines derived from AML patients. These were cells with different mutation status and cytogenetics. The MOLM-13 and MV4-11 cells are from the monocytic lineage, and display heterozygotic and homozygotic internal tandem duplication (ITD) of Flt3, respectively, which both are associated with high risk. The OCI-AML3 cell line has wild-type Flt3, associated with low risk, but a complex karyotype, which turns this cell line into a high-risk model. In line with this, we have found that the OCI-AML3 are more resistant than MOLM-13 and MV4-11 cells to other kinase inhibitors, which did not correspond to expression of drug transporters.[36,37]

The CDK8 inhibitors tested had EC_{50} values between 2.7 μM and 10 μM for the AML cells (Table 1). The analog **13** was the most potent, with values below 4.1 μM for all AML cell lines (Table 1). Interestingly, the analogs did not show significantly different activity towards the three AML cell lines. This suggests that their cell death targets are different from other cytostatics like daunorubicin and kinase inhibitors, which for instance have low activity towards the cytogenetically complex OCI-AML3 cells compared to their activity towards MOLM-13 and MV4-11. The analogs were next tested against the two non-malignant cell lines NRK (rat epithelial kidney cells) and H9c2 (cardio myoblasts) to find if the compounds also could affect normal tissue. In comparison to the malignant cell lines, these cells tolerated two to four times higher concentration of most of the analogs (Table 2).

3. Conclusion

Herein, ten new synthetic compounds have been reported and evaluated for their inhibitory properties towards CDK8. The initial screening of the compounds proved inhibitory effects toward CDK8 at a concentration of 50 nM. For the five most potent compounds, the individual K_d-values toward the same enzyme were determined, which further proved the ability of the compounds to bind to the kinase *in vitro*. The K_d-values of the three most potent compounds are in line or even lower compared to the previous reported CDK8 inhibitors.[9,10,20,24] Additionally, when tested towards a panel of 468 different kinases, the compounds within this study demonstrated a high degree of selective inhibition of CDK8. Compound **14** is a similar analog to what has already been reported by Hatcher and coworkers.[31] By further structure activity relationship studies, we have improved both the affinity and selectivity towards CDK8 for this class of compounds.

Interestingly, the cellular studies identified compound **13** to be the most cytotoxic compound. This observation is in line with the observation done by Corey and coworkers, where several isoquinoline steroidal analogs where tested for their antiangiogenic activity.[38] However, low selectivity of this compound towards the AML cell lines, compared to the non-malignant cell lines, were observed (Table 2). For the most potent CDK8 inhibitor, compound **12**, the EC_{50} values were slightly higher, i.e. it was less cytotoxic towards the AML cell lines (Fig. 3). However, compound **12** proved more selective in killing AML cell lines, compared to compound **13**. The EC_{50} values are three to four times lower for compound **12** towards the AML cell lines compared to the non-malignant cell lines.

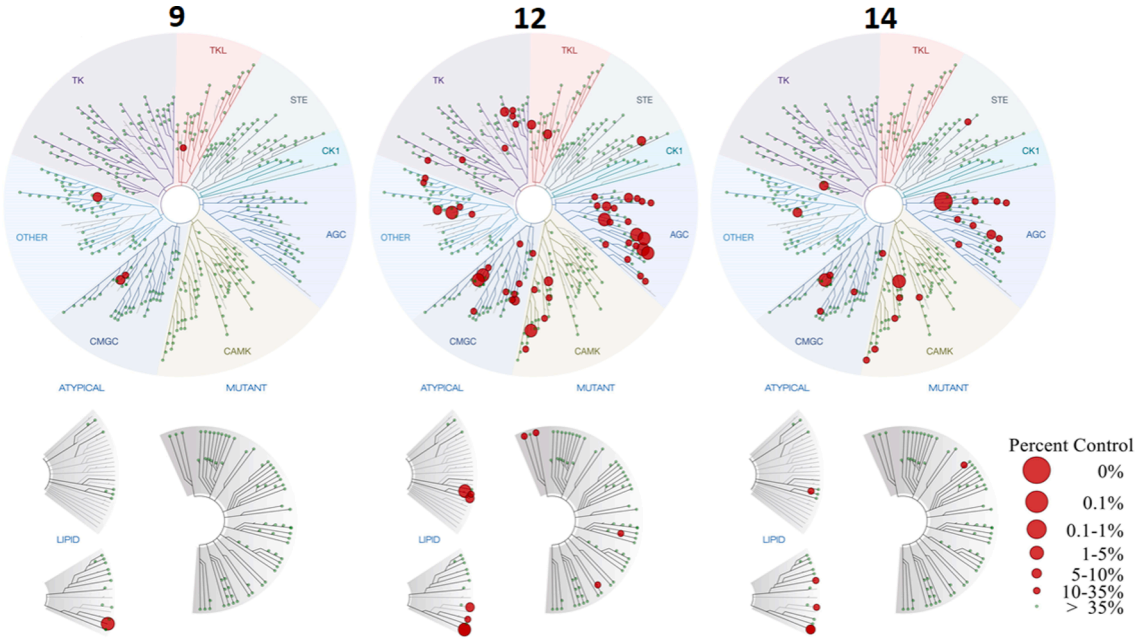

Compound 9	Compound 12			Compound 14
CDK 8	ACVR1	BIKE	CDK11	CDK11
CDK 11	CDK7	CDK8	CLK4	CDK8
IKK-epsilon	FLT4	GRK4	HASPIN	CIT
PIP5K2C	IRAK3	LATS1	MAK	HASPIN
RIPK1	MAP3K2	MET(Y1235D)	p38-delta	HUNK
	PIKFYVE	PIM2	PIP5K1A	MAK
	PIP5K2B	PKAC-alpha	PKAC-beta	PIKFYVE
	PLK4	PRKCQ	PRKG1	PIM2
	PRKG2	RIOK1	RIOK2	PKAC-alpha
	RIOK3	ROCK1	ROCK2	PKAC-beta
	SNARK	SRPK3	TNK1	PYK2
	TRKA	YANK1	TNK1	
	YANK3			

Fig. 2. Tree spot interaction map for compounds **9**, **12** and **14** tested at 50 nM concentrations of inhibitors against 468 wild type and mutant human protein and lipid kinases (KINOMEscan, Eurofins). Kinases where probe binding was inhibited by > 80% at 50 nM test compound concentration are listed.

Table 1
Results from *in vitro* CDK8-evaluation of compounds **8**–**17**.

Compound	CDK8 *per cent of control (POC)*	K_d (nM)	Selectivity score (S10)
8	18%	41	n.d.
9	0%	13	0.02
10	49%	n.d.	n.d.
11	4.3%	n.d.	n.d.
12	0%	3.5	0.14
13	7.3%	45	n.d.
14	0%	18	0.07
15	68%	n.d.	n.d.
16	100%	n.d.	n.d.
17	83%	n.d.	n.d.

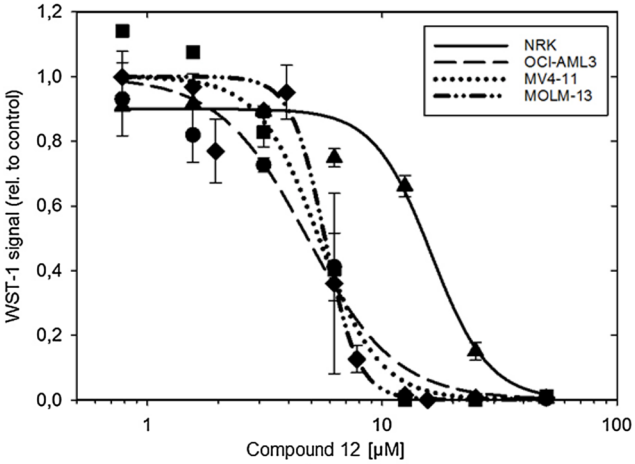

Fig. 3. The cytotoxic effect of compound **12** on the AML cell lines MOLM-13, OCI-AML and MV4-11 as well as the non-cancerous NRK cell line. The cells were exposed to various doses of **12** for 48 h and the metabolic activity of the cells was assessed by the WST-1 assay. The data are average of two–four experiments and standard error. The lines are from four-parameter regression analyses. For experimental details see the experimental section.

4. Experimental

4.1. General methods – Chemistry

All reagents and solvents were used as purchased without further purification unless stated otherwise. Melting points are uncorrected. Analytical TLC was performed using silica gel 60 F254 aluminum plates (Merck). Flash column chromatography was performed on silica gel 60

Table 2
EC_{50} (μM) values of the indicated CDK8 inhibitors on MOLM-13, OCI-AML3, MV4-11, NRK and H9c2 cells after 48 h of incubation with the compounds. The data are based on regression analyses from three experiments. For H9c2, the range for EC_{50} is given, since cells produced data that did not fit to Eq. (1) given in the methods section.

Compound	MOLM-13	OCI-AML3	MV4-11	NRK	H9c2
8	10.2	10.0	10.1	29.7	25–50
9	11.2	7.5	8.6	20.5	12.5–25
12	5.9	4.8	5.4	16.2	12.5–25
13	3.9	2.7	4.1	7.1	6.5–12.5
14	9.0	7.6	5.5	11.4	12.5–25

(40e63 mm) produced by Merck. NMR spectra were recorded on a Bruker Avance DPX-300 MHz, DPX-400 MHz or DPX-600 MHz spectrometer for 1H NMR, and 75 MHz, 101 MHz or 151 MHz for 13C NMR. Coupling constants (J) are reported in hertz, and chemical shifts are reported in parts per million relative to $CDCl_3$ (7.26 ppm for 1H and 77.0 ppm for 13C). Mass spectra were recorded at 70 eV with Fison's VG Pro spectrometer. High-resolution mass spectra were performed with a VG Prospec mass spectrometer and with a Micromass Q-TOF-2™.

*4.2. (3R,5S,8R,9S,10S,13S,14S)-3-azido-10,13-dimethylhexadecahydro-17H-cyclopenta[a]phenanthren-17-one (**5**)*

To a solution of PPh_3 (4.33 g, 16.5 mmol, 1.1 equiv) in THF (90 mL) was added diethyl azodicarboxylate (3.54 mL, 18.0 mmol, 1.2 equiv) at 0 °C and the solution was stirred for 10 min. To this solution epiandrosterone (4.36 g, 15 mmol, 1 equiv) was added. After stirring for an additional 10 min, diphenylphosphoryl azide (3.87 mL, 18.0 mmol, 1.2 equiv) was added slowly. The reaction mixture was allowed to warm to room temperature. After 10 h, 0.1 M NaOH was added and the resulting mixture extracted with 5 × 50 mL DCM. The combined organic layers were dried over $MgSO_4$, evaporated and the compound was purified by flash chromatography (SiO_2, 30% EtOAc in heptane) to afford the product in 73% yield. ^{1}H NMR (400 MHz, $CDCl_3$) δ 4.05–3.67 (m, 1H), 2.56–2.33 (m, 1H), 2.14–2.00 (m, 1H), 1.98–1.88 (m, 1H), 1.84–1.62 (m, 5H), 1.59–1.38 (m, 6H), 1.33–1.16 (m, 6H), 1.02 (qd, J = 12.4, 4.8 Hz, 1H), 0.89–0.74 (m, 7H). ^{13}C NMR (101 MHz, $CDCl_3$) δ 58.04, 54.25, 51.45, 47.77, 40.04, 36.06, 35.82, 35.02, 32.82, 32.51, 31.53, 30.72, 27.99, 25.59, 21.73, 20.04, 13.82, 11.57.

*4.3. (3R,5S,8R,9S,10S,13S,14S)-3-(dimethylamino)-10,13-dimethylhexadecahydro-17H-cyclopenta[a]phenanthren-17-one (**6**)*

A solution of azido steroid **5** (2.16 g, 6 mmol, 1 equiv) in a mixture of THF (6 mL) and aqueous NaOH (1.0 M, 3 mL) was degassed by purging for 20 min with a slow stream of argon gas through a 20-gauge stainless steel needle. To the degassed solution was added a solution of trimethylphosphine in THF (1.0 M, 18 mL, 18 mmol, 3 equiv). After 2 h, MeOH (90 mL) was added, followed by aqueous HCl (4.0 M, 5 mL), and then acetic acid (6.86 mL, 120 mmol, 20 equiv). To the resulting solution were added sequentially formalin (37%wt, 11.05 mL, 300 mmol, 50 equiv) and a solution of sodium cyanoborohydride (3.77 g, 60 mmol, 10 equiv) in MeOH (1 mL). After 1 h, the reaction mixture was concentrated to remove the bulk of the solvent. The concentrate was partitioned between aqueous NaOH (1.0 M, 20 mL) and DCM (40 mL). The layers were separated. The aqueous layer was extracted with DCM (4 × 20 mL). The organic layers were combined, and washed with saturated aqueous sodium chloride solution (30 mL). The combined organic layers was dried over sodium sulfate, evaporated and purified by flash chromatography (SiO_2, 10% MeOH in DCM; SiO_2 was pretreated with 1% Et_3N in $CHCl_2$). ^{1}H NMR (400 MHz, $CDCl_3$) δ 2.46–2.34 (m, 1H), 2.20 (s, 6H), 2.09–1.96 (m, 2H), 1.95–1.69 (m, 4H), 1.67–1.14 (m, 14H), 1.10–0.95 (m, 1H), 0.94–0.85 (m, 1H), 0.83 (s, 3H), 0.81 (s, 3H). ^{13}C NMR (101 MHz, $CDCl_3$) δ 221.50, 61.72, 54.43, 51.67, 47.97, 43.97, 39.67, 36.42, 35.95, 35.20, 33.12, 31.90, 31.72, 30.90, 28.56, 25.00, 21.87, 20.19, 13.96, 12.21.

*4.4. (3R,5S,8R,9S,10S,13S,14S)-3-(dimethylamino)-10,13-dimethyl-2,3,4,5,6,7,8,9,10,11,12,13,14,15-tetradecahydro-1H-cyclopenta[a]phenanthren-17-yl trifluoromethanesulfonate (**7**)*

Dimethylamino steroid **6** (2.22 g, 7.0 mmol) and *N*-phenylbis(trifluoromethanesulfonimide) (3.75 g, 10.5 mmol) were dissolved in dry THF (70 mL) and cooled to −78 °C. NaHMDS (14 mL 1.0 M in THF, 14 mmol), was added dropwise at −78 °C and the resulting mixture was stirred at −78 °C for 10 h. Then the reaction was brought to room temperature and quenched by addition of saturated aqueous NH_4Cl (20 mL). The mixture was extracted with CH_2Cl_2 (4 × 30 mL); the combined organic extracts were washed with water and brine, dried ($MgSO_4$) and concentrated *in vacuo*. The residue was purified by flash chromatography (SiO_2, 2% MeOH in DCM; SiO_2 was pretreated with 1% Et_3N in $CHCl_2$).) to afford the product in 85% yield. ^{1}H NMR (400 MHz, $CDCl_3$) δ 5.54 (dd, J = 3.3, 1.7 Hz, 1H), 2.29–2.11 (m, 7H), 2.03 (s, 1H), 2.00–1.90 (m, 1H), 1.87–1.78 (m, 1H), 1.75–1.43 (m, 8H), 1.42–1.16 (m, 7H), 1.08–0.91 (m, 5H), 0.84 (s, 3H). ^{13}C NMR (101 MHz, $CDCl_3$) δ 159.39, 118.57 (q, J = 320.42 Hz), 114.28, 99.99, 77.34, 77.22, 77.02, 76.70, 61.63, 54.54, 54.32, 44.92, 43.85, 39.71, 36.38, 33.92, 33.49, 32.74, 32.72, 31.71, 30.70, 28.53, 28.41, 24.79, 20.11, 20.09, 15.30, 12.09, 12.03, 0.09.

*4.5. General procedure for the Suzuki cross-coupling (**8**–**17**)*

The dimethylamino steroid triflate (0.2 mmol, 1 equiv.), cesium carbonate (2 equiv.) and the boronic acid (1.05 equiv.) were placed in a 50 mL round-bottomed flask under an argon atmosphere and dissolved in a 1:1 mixture of water and THF. $Pd(PPh_3)_4$ (5%mol) was added and the reaction mixture was stirred at room temperature (18–22 h.). Upon completion the reaction mixture was poured into brine (15 mL) and extracted with ethyl acetate (4 × 5 mL). The combined organic extracts were dried ($MgSO_4$) and the solvent evaporated *in vacuo*. The residue was purified by flash chromatography (silica gel, 10% MeOH in DCM; SiO_2 was pretreated with 1% Et_3N in $CHCl_2$) to give the pure products.

*4.6. (3R,5S,8R,9S,10S,13S,14S)-N,N,10,13-tetramethyl-17-(pyridin-3-yl)-2,3,4,5,6,7,8,9,10,11,12,13,14,15-tetradecahydro-1H-cyclopenta[a]phenanthren-3-amine (**8**)*

The compound was prepared following the general procedure described. The product was isolated as colorless solid (63 mg, 83%). ^{1}H NMR (400 MHz, $CDCl_3$) δ 8.58 (d, J = 2.5 Hz, 1H), 8.42 (d, J = 6.3 Hz, 1H), 7.70–7.53 (m, 1H), 7.22–7.11 (m, 1H), 5.94 (dd, J = 3.3, 1.8 Hz, 1H), 2.43 (s, 6H), 2.26–2.08 (m, 1H), 2.05–1.82 (m, 3H), 1.75–1.66 (m, 2H), 1.66–1.54 (m, 5H), 1.52–1.33 (m, 5H), 1.29–1.01 (m, 5H), 0.98 (s, 3H), 0.86 (s, 3H). ^{13}C NMR (101 MHz, $CDCl_3$) δ 151.91, 148.00, 147.83, 133.87, 133.23, 129.33, 123.10, 62.66, 57.41, 54.02, 47.71, 43.56, 39.58, 36.37, 35.38, 34.15, 32.63, 31.78, 31.60, 31.03, 28.64, 24.26, 20.88, 16.84, 12.17. HRMS (EI): Exact mass calculated for $C_{28}H_{38}N_2$ $[M+H]^+$: 379.3069, found 379.3108.

*4.7. (3R,5S,8R,9S,10S,13S,14S)-17-(5-chloropyridin-3-yl)-N,N,10,13-tetramethyl-2,3,4,5,6,7,8,9,10,11,12,13,14,15-tetradecahydro-1H-cyclopenta[a]phenanthren-3-amine (**9**)*

The compound was prepared following the general procedure described. The product was isolated as colorless solid (57 mg, 69%). ^{1}H NMR (400 MHz, $CDCl_3$) δ 8.47 (d, J = 1.9 Hz, 1H), 8.40 (d, J = 2.4 Hz, 1H), 7.61 (t, J = 2.1 Hz, 1H), 6.12–5.87 (m, 1H), 2.91 (s, 1H), 2.78 (s, 6H), 2.33–2.15 (m, 1H), 2.10–1.91 (m, 3H), 1.85–1.77 (m, 1H), 1.77–1.69 (m, 1H), 1.68–1.58 (m, 6H), 1.57–1.48 (m, 2H), 1.45–1.40

(m, 2H), 1.32–1.21 (m, 2H), 1.21–1.05 (m, 2H), 0.98 (s, 3H), 0.88 (s, 3H). ^{13}C NMR (101 MHz, $CDCl_3$) δ 150.52, 146.63, 145.74, 134.35, 133.49, 131.70, 130.98, 64.26, 57.05, 53.30, 47.68, 43.19, 39.24, 36.21, 35.09, 33.97, 31.81, 31.16, 29.81, 28.33, 23.27, 20.81, 16.88, 12.03. HRMS (EI): Exact mass calculated for $C_{28}H_{37}ClN_2$ $[M+H]^+$: 414.2616, found 414.2657.

*4.8. (3R,5S,8R,9S,10S,13S,14S)-N,N,10,13-tetramethyl-17-(pyridin-4-yl)-2,3,4,5,6,7,8,9,10,11,12,13,14,15-tetradecahydro-1H-cyclopenta[a]phenanthren-3-amine (**10**)*

The compound was prepared following the general procedure described. The product was isolated as colorless solid (85 mg, 64%). ^{1}H NMR (400 MHz, $CDCl_3$) δ 8.47 (d, J = 5.2 Hz, 1H), 7.23 (d, J = 6.1 Hz, 2H), 6.12 (dd, J = 3.4, 1.8 Hz, 1H), 2.36 (s, 6H), 2.27–2.18 (m, 2H), 2.07–1.95 (m, 2H), 1.91–1.82 (m, 1H), 1.77–1.51 (m, 8H), 1.40 (d, J = 8.6 Hz, 5H), 1.30–1.20 (m, 3H), 1.15–1.07 (m, 1H), 1.01 (s, 3H), 0.86 (s, 3H). ^{13}C NMR (101 MHz, $CDCl_3$) δ 152.60, 149.59, 144.67, 131.43, 121.17, 62.24, 57.37, 54.04, 47.39, 43.58, 39.52, 36.27, 35.18, 33.94, 32.61, 31.68, 31.52, 31.21, 28.54, 24.39, 20.73, 16.76, 12.05. HRMS (EI): Exact mass calculated for $C_{28}H_{38}N_2$ $[M+H]^+$: 379.3069, found 379.3108.

*4.9. (3R,5S,8R,9S,10S,13S,14S)-17-(isoquinolin-4-yl)-N,N,10,13-tetramethyl-2,3,4,5,6,7,8,9,10,11,12,13,14,15-tetradecahydro-1H-cyclopenta[a]phenanthren-3-amine (**11**)*

The compound was prepared following the general procedure described. The product was isolated as colorless solid (62 mg, 72%). ^{1}H NMR (400 MHz, $CDCl_3$) δ 9.13 (s, 1H), 8.29 (s, 1H), 7.96 (dd, J = 25.9, 8.1 Hz, 2H), 7.73–7.52 (m, 2H), 5.80 (s, 1H), 2.56 (s, 6H), 2.37 (d, J = 14.4 Hz, 1H), 2.14 (t, J = 13.2 Hz, 1H), 1.83 (dd, J = 23.8, 13.2 Hz, 4H), 1.53 (s, 6H), 1.45–1.32 (m, 2H), 1.25 (dd, J = 14.2, 7.3 Hz, 7H), 0.95 (s, 3H), 0.85 (s, 4H). ^{13}C NMR (101 MHz, $CDCl_3$) δ 151.20, 149.80, 141.64, 135.54, 131.57, 129.99, 129.37, 128.38, 127.46, 126.91, 125.69, 62.99, 58.19, 56.98, 53.80, 49.75, 43.18, 39.28, 36.25, 34.80, 34.45, 32.26, 32.23, 31.50, 30.42, 28.47, 23.71, 18.46, 12.00. HRMS (EI): Exact mass calculated for $C_{30}H_{40}N_2$ $[M+H]^+$: 429.3225, found 429.3264.

*4.10. (3R,5S,8R,9S,10S,13S,14S)-17-(isoquinolin-5-yl)-N,N,10,13-tetramethyl-2,3,4,5,6,7,8,9,10,11,12,13,14,15-tetradecahydro-1H-cyclopenta[a]phenanthren-3-amine (**12**)*

The compound was prepared following the general procedure described. The product was isolated as colorless solid (60 mg, 70%). ^{1}H NMR (400 MHz, $CDCl_3$) δ 9.19 (s, 1H), 8.47 (d, J = 6.0 Hz, 1H), 7.94–7.79 (m, 2H), 7.59–7.52 (m, 1H), 7.45 (dd, J = 7.2, 1.2 Hz, 1H), 5.80–5.67 (m, 1H), 2.58 (s, 6H), 2.41–2.30 (m, 1H), 2.21–2.08 (m, 1H), 1.97–1.74 (m, 4H), 1.71–1.15 (m, 15H), 0.92 (s, 3H), 0.85 (s, 3H). ^{13}C NMR (101 MHz, $CDCl_3$) δ 152.49, 151.17, 142.88, 135.42, 135.15, 130.72, 129.51, 128.95, 126.38, 126.27, 119.33, 63.10, 56.98, 53.74, 49.69, 43.15, 39.27, 36.25, 34.91, 34.41, 32.22, 32.15, 31.46, 30.34, 28.46, 23.64, 20.72, 16.48, 12.01. HRMS (EI): Exact mass calculated for $C_{30}H_{40}N_2$ $[M+H]^+$: 429.3225, found 429.3264.

*4.11. (3R,5S,8R,9S,10S,13S,14S)-17-(isoquinolin-6-yl)-N,N,10,13-tetramethyl-2,3,4,5,6,7,8,9,10,11,12,13,14,15-tetradecahydro-1H-cyclopenta[a]phenanthren-3-amine (**13**)*

The compound was prepared following the general procedure described. The product was isolated as colorless solid (68 mg, 79%). ^{1}H NMR (400 MHz, $CDCl_3$) δ 9.16 (s, 1H), 8.46 (d, J = 5.9 Hz, 1H), 7.85 (d, J = 8.6 Hz, 1H), 7.73 (d, J = 1.7 Hz, 1H), 7.67–7.56 (m, 2H), 6.10 (dd, J = 3.2, 1.7 Hz, 1H), 2.74 (s, 1H), 2.64 (s, 6H), 2.31–2.19 (m, 1H), 2.15–1.86 (m, 3H), 1.79–1.32 (m, 13H), 1.31–1.21 (m, 2H), 1.07 (s, 4H), 0.87 (s, 3H). ^{13}C NMR (101 MHz, $CDCl_3$) δ 154.06, 151.89, 142.96, 139.43, 135.95, 130.40, 127.55, 127.24, 127.22, 122.85, 120.69, 63.43, 57.27, 53.55, 47.62, 43.13, 39.30, 36.11, 35.33, 33.90, 31.99, 31.71, 31.25, 30.06, 28.31, 23.43, 20.77, 16.85, 11.95. HRMS (EI): Exact mass calculated for $C_{30}H_{40}N_2$ $[M+H]^+$: 429.3225, found 429.3264.

*4.12. (3R,5S,8R,9S,10S,13S,14S)-17-(isoquinolin-7-yl)-N,N,10,13-tetramethyl-2,3,4,5,6,7,8,9,10,11,12,13,14,15-tetradecahydro-1H-cyclopenta[a]phenanthren-3-amine (**14**)*

The compound was prepared following the general procedure described. The product was isolated as colorless solid (65 mg, 76%). ^{1}H NMR (400 MHz, $CDCl_3$) δ 9.19 (s, 1H), 8.44 (d, J = 5.7 Hz, 1H), 7.87 (d, J = 1.5 Hz, 1H), 7.72 (d, J = 1.2 Hz, 2H), 7.58 (d, J = 5.6 Hz, 1H), 6.05 (dd, J = 3.3, 1.7 Hz, 1H), 2.96 (s, 1H), 2.77 (s, 6H), 2.30–2.17 (m, 1H), 2.14–2.07 (m, 1H), 2.06–1.92 (m, 2H), 1.84–1.69 (m, 2H), 1.69–1.56 (m, 7H), 1.47–1.34 (m, 3H), 1.31–1.21 (m, 3H), 1.25–1.13 (m, 1H), 1.07 (s, 3H), 0.88 (s, 3H). ^{13}C NMR (101 MHz, $CDCl_3$) δ 153.90, 152.54, 142.53, 136.36, 134.69, 130.32, 129.23, 128.78, 126.13, 123.90, 120.18, 63.98, 57.15, 53.30, 47.57, 42.94, 39.19, 36.08, 35.31, 33.88, 31.72, 31.59, 31.11, 29.63, 28.22, 23.08, 20.77, 16.81, 11.89. HRMS (EI): Exact mass calculated for $C_{30}H_{40}N_2$ $[M+H]^+$: 429.3225, found 429.3262.

*4.13. (3R,5S,8R,9S,10S,13S,14S)-17-(1H-indol-4-yl)-N,N,10,13-tetramethyl-2,3,4,5,6,7,8,9,10,11,12,13,14,15-tetradecahydro-1H-cyclopenta[a]phenanthren-3-amine (**15**)*

The compound was prepared following the general procedure described. The product was isolated as colorless solid (59 mg, 71%). ^{1}H NMR (400 MHz, $CDCl_3$) δ 8.58–8.17 (m, 1H), 7.27 (d, J = 7.9 Hz, 1H), 7.16 (t, J = 2.8 Hz, 1H), 7.12 (t, J = 7.7 Hz, 1H), 7.04–6.98 (m, 1H), 6.64 (t, J = 2.9 Hz, 1H), 5.99 (dd, J = 3.2, 1.7 Hz, 1H), 2.39 (s, 6H), 2.34–2.26 (m, 2H), 2.13–2.02 (m, 1H), 1.92–1.80 (m, 2H), 1.79–1.72 (m, 1H), 1.69–1.22 (m, 14H), 1.19–1.08 (m, 1H), 1.03 (s, 3H), 0.86 (s, 3H). ^{13}C NMR (101 MHz, $CDCl_3$) δ 153.57, 136.04, 130.26, 128.48, 127.33, 123.75, 121.34, 118.12, 109.66, 103.01, 62.51, 57.25, 54.26, 48.64, 43.52, 39.65, 36.29, 35.48, 34.23, 32.57, 31.94, 31.69, 31.04, 28.64, 24.21, 20.84, 17.01, 12.07. HRMS (EI): Exact mass calculated for $C_{29}H_{40}N_2$ $[M+H]^+$: 417.3225, found 417.3265.

*4.14. (3R,5S,8R,9S,10S,13S,14S)-17-(1H-indol-5-yl)-N,N,10,13-tetramethyl-2,3,4,5,6,7,8,9,10,11,12,13,14,15-tetradecahydro-1H-cyclopenta[a]phenanthren-3-amine (**16**)*

The compound was prepared following the general procedure described. The product was isolated as colorless solid (55 mg, 66%). ^{1}H NMR (400 MHz, $CDCl_3$) δ 8.37 (s, 1H), 7.69–7.60 (m, 1H), 7.32–7.27 (m, 1H), 7.25–7.22 (m, 1H), 7.15 (dd, J = 3.2, 2.3 Hz, 1H), 6.57–6.48 (m, 1H), 5.88–5.74 (m, 1H), 2.29 (s, 6H), 2.24–2.15 (m, 1H), 2.13–2.05 (m, 2H), 2.03–1.93 (m, 1H), 1.89–1.80 (m, 1H), 1.76–1.68 (m, 1H), 1.69–1.50 (m, 6H), 1.46–1.32 (m, 5H), 1.28–1.20 (m, 2H), 1.14–1.07 (m, 1H), 1.05 (s, 3H), 0.95 (dd, J = 11.9, 10.0 Hz, 1H), 0.88 (s, 3H). ^{13}C NMR (101 MHz, $CDCl_3$) δ 156.04, 135.09, 129.47, 127.90, 125.35, 124.48, 121.87, 118.66, 110.71, 102.86, 62.05, 57.76, 54.54, 47.71, 43.93, 39.90, 36.46, 35.86, 34.29, 32.99, 31.89, 31.83, 31.58, 28.89, 24.91, 21.01, 16.97, 12.24. HRMS (EI): Exact mass calculated for $C_{29}H_{40}N_2$ $[M+H]^+$: 417.3225, found 417.3264.

*4.15. (3R,5S,8R,9S,10S,13S,14S)-17-(1H-indol-6-yl)-N,N,10,13-tetramethyl-2,3,4,5,6,7,8,9,10,11,12,13,14,15-tetradecahydro-1H-cyclopenta[a]phenanthren-3-amine (**17**)*

The compound was prepared following the general procedure described. The product was isolated as colorless solid (53 mg, 64%). ^{1}H

NMR (400 MHz, $CDCl_3$) δ 8.28 (s, 1H), 7.54 (d, J = 8.2 Hz, 1H), 7.43–7.36 (m, 1H), 7.22–7.09 (m, 2H), 6.63–6.36 (m, 1H), 5.87 (dd, J = 3.2, 1.7 Hz, 1H), 2.31 (s, 6H), 2.24–2.17 (m, 1H), 2.16–2.13 (m, 1H), 2.12–2.07 (m, 1H), 2.04–1.93 (m, 1H), 1.90–1.81 (m, 1H), 1.77–1.70 (m, 1H), 1.68–1.50 (m, 6H), 1.48–1.33 (m, 5H), 1.29–1.21 (m, 2H), 1.17–1.08 (m, 1H), 1.05 (s, 3H), 1.02–0.95 (m, 1H), 0.88 (s, 3H). ^{13}C NMR (101 MHz, $CDCl_3$) δ 155.77, 135.97, 131.57, 126.73, 125.94, 124.30, 120.06, 119.62, 108.99, 102.41, 62.04, 57.65, 54.39, 47.62, 43.74, 39.75, 36.34, 35.77, 34.16, 32.82, 31.73, 31.55, 31.49, 28.72, 24.66, 20.91, 16.91, 12.11. HRMS (EI): Exact mass calculated for $C_{29}H_{40}N_2$ $[M+H]^+$: 417.3225, found 417.3264.

4.16. Protein kinase assay

For the CDK8 and CDK11 profiling we used a kinase selectivity and profiling assay (DiscoveRx).[39] The assay uses kinase-tagged T7 phage strains which were grown in parallel in 24-well blocks in an *E. coli* host derived from the BL21 strain. *E. coli* were grown to log-phase and infected with T7 phage from a frozen stock (multiplicity of infection = 0.4) and incubated with shaking at 32 °C until lysis (90–150 min). The lysates were centrifuged (6000*g*) and filtered (0.2 μm) to remove cell debris. Streptavidin-coated magnetic beads were treated with biotinylated small molecule ligands for 30 min at room temperature to generate affinity resins for kinase assays. The liganded beads were blocked with excess biotin and washed with blocking buffer (SeaBlock (Pierce), 1% BSA, 0.05% Tween 20, 1 mM DTT) to remove unbound ligand and to reduce non-specific phage binding. Binding reactions were assembled by combining kinases, liganded affinity beads, and test compounds in 1x binding buffer (20% SeaBlock, 0.17x PBS, 0.05% Tween 20, 6 mM DTT). Test compounds were prepared as 40x stocks in 100% DMSO and directly diluted into the assay. All reactions were performed in polypropylene 384-well plates in a final volume of 20 μL. The assay plates were incubated at room temperature with shaking for 1 h and the affinity beads were washed with wash buffer (1x PBS, 0.05% Tween 20). The beads were then re-suspended in elution buffer (1x PBS, 0.05% Tween 20, 0.5 μM non-biotinylated affinity ligand) and incubated at room temperature with shaking for 30 min. The kinase concentration in the eluates was measured by qPCR. The test compounds were screened at 50 nM, and results for primary screen binding interactions are reported as POC (percent of control). The negative control consists of adding an equal DMSO volume without a test compound and the positive control consist of a control compound. From this POC is calculated: ((test compound signal − positive control signal)/(negative control signal − positive control signal)) × 100%. Negative control = DMSO (100% Ctrl); Positive control = control compound (0% Ctrl), where lower numbers indicate stronger hits in the matrix.

For the binding constant (K_d) determination an 11-point 3-fold serial dilution of each test compound was prepared in 100% DMSO at 100x final test concentration and subsequently diluted to 1x in the assay (final DMSO concentration = 1%). Most K_d values were determined using a compound top concentration = 30,000 nM. The K_d values were calculated with a standard dose-response curve using the Hill equation and are expressed as an average of two determinations.

4.17. Cell growth inhibition (cytotoxicity)

All cell culturing media and serum were from Sigma-Aldrich (St. Louis, MO, USA). The human acute myeloid leukemia (AML) cell lines MOLM-13 (ACC: 554,[40]) and OCI-AML3 (ATCC, ACC-528) were cultured in RPMI medium (R5886) enriched with 10% fetal bovine serum (F7524) and 2 mM L-glutamine (G7513). The human AML cell line MV4-11 (ATCC, CRL-9591) was cultured in Iscove medium (I3390) enriched with 10% fetal bovine serum (F7524) and 8 mM L-glutamine (G7513). The normal rat kidney epithelial (NRK, ATCC, CRL-6509) and the rat cardiomyoblast (H9c2, ATCC, CRL-1446) cells were cultured in DMEM medium (D6429) enriched with 10% fetal bovine serum (F7524). All cell lines were additionally supplemented with 100 IU/mL penicillin and 100 μg/mL streptomycin (P0781). The cells were cultured in a humidified atmosphere under 20% O_2 at 37 °C.

All analogs were dissolved in DMSO (D5879, Sigma-Aldrich) to a stock concentration of 25 mM before testing, and stored at −80 °C. For cytotoxic testing, the three AML cell lines were seeded at 10,000 cells/well, while NRK cells were seeded as 2000 cells/well and H9c2 as 2500 cells/well in 96-well Microplates (#167008, Thermo Scientific™ Nunc™ MicroWell™) with 0.1 mL medium/well. The cells were exposed to various concentrations of CDK8 inhibitors for 48 h before the cell proliferation reagent WST-1 (11644807001, Roche Diagnostics, Sigma-Aldrich) was used to assess the viability, in accordance with the manufacturer's instructions. The cells were next fixed in 2% buffered formaldehyde (pH 7.4) with the DNA-specific dye Hoechst 33,342 (Polysciences Inc.) and assessed for cell death by UV-microscopy based on nuclear morphology. Viability assessment with these two methods is shown to correlate well with cells exposed to kinase inhibitors[37].

EC_{50} values were determined based on data from WST-1 assay in combination with microscopic evaluation of cell death, using four-parameter regression analysis function in the SigmaPlot software (Systat Software inc. San Jose, CA):

$$Y = min + \frac{(max - min)}{1 + \left(\frac{X}{EC50}\right)^h} \quad (1)$$

where Y is the response (WST-1 signal or percent apoptosis), min and max are minimum and maximum response, X is concentration of analog, EC50 equals the point of inflection, i.e. the point that gives half of maximum response, and h is the Hill's slope of the curve.

Declaration of Competing Interest

The authors declare that they have no known competing financial interests or personal relationships that could have appeared to influence the work reported in this paper.

Acknowledgement

Faculty of Health sciences, Nord University are gratefully acknowledged for financial support of the project. Reidun Aesoy and Lars Herfindal received financial support from NordForsk (NCoE Programme "NordAqua" (project #82845)), Western Norway Health Authorities, and the Norwegian Society for Children's Cancer.

Appendix A. Supplementary material

Supplementary data to this article can be found online at https://doi.org/10.1016/j.bmc.2020.115461.

References

1. Malumbres M. Cyclin-dependent kinases. *Genome Biol.* 2014;15:122.
2. Tassan JP, Jaquenoud M, Léopold P, Schultz SJ, Nigg EA. Identification of human cyclin-dependent kinase 8, a putative protein kinase partner for cyclin C. *Proc Natl Acad Sci.* 1995;92:8871.
3. Poss ZC, Ebmeier CC, Taatjes DJ. The mediator complex and transcription regulation. *Crit Rev Biochem Mol Biol.* 2013;48:575–608.
4. Donner AJ, Szostek S, Hoover JM, Espinosa JM. CDK8 Is a stimulus-specific positive coregulator of p53 target genes. *Mol Cell.* 2007;27:121–133.
5. Firestein R, Bass AJ, Kim SY, et al. CDK8 is a colorectal cancer oncogene that regulates [bgr]-catenin activity. *Nature.* 2008;455:547–551.
6. Grasso CS, Wu Y-M, Robinson DR, et al. The mutational landscape of lethal castration-resistant prostate cancer. *Nature.* 2012;487:239–243.
7. Kapoor A, Goldberg MS, Cumberland LK, et al. The histone variant macroH2A suppresses melanoma progression through regulation of CDK8. *Nature.* 2010;468:1105–1109.
8. Eirew P, Steif A, Khattra J, et al. Dynamics of genomic clones in breast cancer patient xenografts at single-cell resolution. *Nature.* 2015;518:422–426.
9. Porter DC, Farmaki E, Altilia S, et al. Cyclin-dependent kinase 8 mediates

chemotherapy-induced tumor-promoting paracrine activities. *Proc Natl Acad Sci.* 2012;109:13799–13804.
10. Rzymski T, Mikula M, Zylkiewicz E, et al. SEL120-34A is a novel CDK8 inhibitor active in AML cells with high levels of serine phosphorylation of STAT1 and STAT5 transactivation domains. *Oncotarget.* 2017;8:33779–33795.
11. Wingelhofer B, Maurer B, Heyes EC, et al. Pharmacologic inhibition of STAT5 in acute myeloid leukemia. *Leukemia.* 2018;32:1135–1146.
12. Konig H, Levis M. Targeting FLT3 to treat leukemia. *Expert Opin Therapeutic Targets.* 2015;19:37–54.
13. Putz EM, Gotthardt D, Hoermann G, et al. CDK8-mediated STAT1-S727 phosphorylation restrains NK cell cytotoxicity and tumor surveillance. *Cell Rep.* 2013;4:437–444.
14. Witalisz-Siepracka A, Gotthardt D, Prchal-Murphy M, et al. V. Sexl, NK Cell-Specific CDK8 deletion enhances antitumor responses. *Cancer Immunol Res.* 2018.
15. Shallal HM, Russu WA. Discovery, synthesis, and investigation of the antitumor activity of novel piperazinylpyrimidine derivatives. *Eur J Med Chem.* 2011;46:2043–2057.
16. Palmer WS, Alam M, Arzeno HB, et al. Development of amino-pyrimidine inhibitors of c-Jun N-terminal kinase (JNK): Kinase profiling guided optimization of a 1,2,3-benzotriazole lead. *Bioorg Med Chem Lett.* 2013;23:1486–1492.
17. Getlik M, Grütter C, Simard JR, et al. Hybrid compound design to overcome the gatekeeper T338M mutation in cSrc#. *J Med Chem.* 2009;52:3915–3926.
18. Saurat T, Buron F, Rodrigues N, et al. Design, synthesis, and biological activity of pyridopyrimidine scaffolds as novel PI3K/mTOR dual inhibitors. *J Med Chem.* 2014;57:613–631.
19. Aoki S, Watanabe Y, Sanagawa M, Setiawan A, Kotoku N, Kobayashi M. Cortistatins A, B, C, and D, anti-angiogenic steroidal alkaloids, from the marine sponge corticium simplex. *J Am Chem Soc.* 2006;128:3148–3149.
20. Cee VJ, Chen DYK, Lee MR, Nicolaou KC. Cortistatin A is a high-affinity ligand of protein kinases ROCK, CDK8, and CDK11. *Angew. Chemie Int. Ed.* 2009;48:8952–8957.
21. Karaman MW, Herrgard S, Treiber DK, et al. A quantitative analysis of kinase inhibitor selectivity. *Nat Biotechnol.* 2008;26:127.
22. Pelish HE, Liau BB, Nitulescu II, et al. Mediator kinase inhibition further activates super-enhancer-associated genes in AML. *Nature.* 2015;526:273–276.
23. Mallinger A, Crumpler S, Pichowicz M, et al. Discovery of potent, orally bioavailable, small-molecule inhibitors of WNT signaling from a cell-based pathway screen. *J Med Chem.* 2015;58:1717–1735.
24. Dale T, Clarke PA, Esdar C, et al. A selective chemical probe for exploring the role of CDK8 and CDK19 in human disease. *Nat Chem Biol.* 2015;11:973.
25. Solum EJ, Cheng J-J, Sørvik IB, Paulsen RE, Vik A, Hansen TV. Synthesis and biological evaluations of new analogs of 2-methoxyestradiol: Inhibitors of tubulin and angiogenesis. *Eur J Med Chem.* 2014;85:391–398.
26. Solum EJ, Vik A, Hansen TV. Synthesis, cytotoxic effects and tubulin polymerization inhibition of 1,4-disubstituted 1,2,3-triazole analogs of 2-methoxyestradiol. *Steroids.* 2014;87:46–53.
27. Solum EJ, Cheng J-J, Sylte I, Vik A, Hansen TV. Synthesis, biological evaluation and molecular modeling of new analogs of the anti-cancer agent 2-methoxyestradiol: potent inhibitors of angiogenesis. *RSC Adv.* 2015;5:32497–32504.
28. Al-Kazaale N, Tran PT, Haidari F, et al. Synthesis, molecular modeling and biological evaluation of potent analogs of 2-methoxyestradiol. *Steroids.* 2018;136:47–55.
29. Sørvik IB, Solum EJ, Labba NA, Hansen TV, Paulsen RE. Differential effects of some novel synthetic oestrogen analogs on oxidative PC12 cell death caused by serum deprivation. *Free Radical Res.* 2018;52:273–287.
30. Mohamed YMA, El Nazer HA, Solum EJ. Practical synthesis of silyl-protected and functionalized propargylamines using nanostructured Ag/TiO2 and Pt/TiO2 as active recyclable catalysts. *Chem Pap.* 2019;73:435–445.
31. Hatcher JM, Wang ES, Johannessen L, Kwiatkowski N, Sim T, Gray NS. Development of Highly Potent and Selective Steroidal Inhibitors and Degraders of CDK8. *ACS Med Chem Lett.* 2018;9:540–545.
32. Shi J, Shigehisa H, Guerrero CA, Shenvi RA, Li C-C, Baran PS. Stereodivergent Synthesis of 17-α and 17-β-Aryl Steroids: Application and Biological Evaluation of D-Ring Cortistatin Analogues. *Angew Chem Int Ed.* 2009;48:4328–4331.
33. Eschweiler W. Ersatz von an Stickstoff gebundenen Wasserstoffatomen durch die Methylgruppe mit Hülfe von Formaldehyd. *Ber Dtsch Chem Ges.* 1905;38:880–882.
34. Clarke HT, Gillespie HB, Weisshaus SZ. The action of formaldehyde on amines and amino acids1. *J Am Chem Soc.* 1933;55:4571–4587.
35. Solum EJ, Mohamed YMA. Convenient stereoselective synthesis of some 3-aminosteroid scaffolds. *Synth Commun.* 2019;49:1159–1164.
36. Macias RIR, Sanchez-Martin A, Rodriguez-Macias G, et al. Role of drug transporters in the sensitivity of acute myeloid leukemia to sorafenib. *Oncotarget.* 2018;9:28474–28485.
37. Bjørnstad R, Aesoy R, Bruserud Ø, et al. A kinase inhibitor with anti-Pim kinase activity is a potent and selective cytotoxic agent towards acute myeloid leukemia. *Mol Cancer Ther.* 2019 molcanther.1234.2017.
38. Czakó B, Kürti L, Mammoto A, Ingber DE, Corey EJ. Discovery of potent and practical antiangiogenic agents inspired by cortistatin A. *J Am Chem Soc.* 2009;131:9014–9019.
39. Fabian MA, Biggs Iii WH, Treiber DK, et al. A small molecule–kinase interaction map for clinical kinase inhibitors. *Nat Biotechnol.* 2005;23:329.
40. Matsuo Y, MacLeod RAF, Uphoff CC, et al. Two acute monocytic leukemia (AML-M5a) cell lines (MOLM-13 and MOLM-14) with interclonal phenotypic heterogeneity showing MLL-AF9 fusion resulting from an occult chromosome insertion, ins(11;9)(q23;p22p23). *Leukemia.* 1997;11:1469–1477.